Chem Biol Drug Des 2014

Research Article

Discovery, Optimization, and Pharmacophore Modeling of Oleanolic Acid and Analogues as Breast Cancer Cell Migration and Invasion Inhibitors Through Targeting Brk/Paxillin/Rac1 Axis

Heba E. Elsayed[1,2], Mohamed R. Akl[1], Hassan Y. Ebrahim[1], Asmaa A. Sallam[1], Eman G. Haggag[2], Amel M. Kamal[2] and Khalid A. El Sayed[1,*]

[1]Department of Basic Pharmaceutical Sciences, School of Pharmacy, University of Louisiana at Monroe, Monroe, LA 71201, USA
[2]Department of Pharmacognosy, Faculty of Pharmacy, Helwan University, Helwan, Cairo 11795, Egypt
**Corresponding author: Khalid A. El Sayed, elsayed@ulm.edu*

Bioassay-guided fractionation of *Terminalia bentzoe* L. leaves methanol extract identified the known triterpene oleanolic acid (1) as its major breast cancer cell migration inhibitor. Further chemical optimization afforded five new (9–12 and 15) and seven known (4–8, 13, and 14) semisynthetic analogues. All compounds were tested for their ability to inhibit human breast cancer MDA-MB-231 cells migration, proliferation, and invasion. The results revealed that 3-O-[N-(3′-chlorobenzenesulfonyl)-carbamoyl]-oleanolic acid (11) and 3-O-[N-(5′-fluorobenzenesulfonyl)-carbamoyl]-oleanolic acid (12) were the most active hits at low μM concentration. Western blot analysis indicated the activity of 1, 11, and 12 might be related, at least in part, to the suppression of Brk/Paxillin/Rac1 signaling pathway. Pharmacophore modeling study was conducted to better understand the common structural binding epitopes important for the antimigratory activity. The sulfonyl carbamoyl moiety with an optimal bulkiness electron-deficient phenyl ring is associated with improved activity. This study is the first to discover the antimigratory and anti-invasive activities of oleanolic acid and analogues through targeting the Brk/Paxillin/Rac1 axis.

Key words: bioassay-guided, breast cancer, Brk/Paxillin/Rac1 axis, Combretaceae, oleanolic acid, *Terminalia bentzoe* L

Received 8 March 2014, revised 7 May 2014 and accepted for publication 7 June 2014

Breast cancer is the most common malignancy among the female population worldwide (1). The high metastatic ability of some breast cancer phenotypes, including tumor cell dissemination to bones, lungs, or brain, ranked breast cancer as the second leading cause of cancer mortality in women (1,2). Breast cancer metastatic cascade involves complicated events, including cell invasion of the basement membrane, migration through the extracellular matrix, and transport by blood vessels and/or lymphatics to distant organs (3). Targeting molecular signaling pathways underlying cancerous cell migration and invasion is among the promising strategies to control metastatic malignancies.

The vast majority of current anticancer drugs are originated from or inspired by natural entities (4). Natural product secondary metabolites are characterized by their structural novelty and diversity, qualifying them as promising scaffolds for the discovery of new anticancer entities (5). The abundance of bioactive plant metabolites offers the advantage for bioguided investigation of their extracts to identify pure bioactive compounds for further optimization. Plants of genus *Terminalia* (Combretaceae) are native to Africa and are widely distributed in tropical and subtropical regions (6). They are known as a rich source of diverse bioactive secondary metabolites, including phenolics and triterpenes (7,8). *Terminalia bentzoe* L. is a medium-sized tree, which is neither chemically nor biologically studied, except for its essential oil content (9).

Oleanolic acid (**1**) is a pentacyclic triterpene widely distributed in food and traditional herbal remedies and exhibits diverse therapeutic effects (10). The anticancer activity of **1** was reported to be mediated through different mechanisms including the inhibition of mitogen-activated protein kinase/extracellular signal-regulated kinase (MAPK/ERK) pathway and inhibition of topoisomerases I and II (11,12). Oleanolic acid has been subjected to various chemical modifications to uncover its structure–activity relationship and optimize its anticancer effect. Various substituents were linked at different positions, while the pentacyclic core skeleton was retained. Examples of prior **1** modification are the derivatizations of C-3 hydroxyl with acids bearing different aliphatic and heterocyclic side chains, which showed improved antitumor activities (13). Other examples include the 2-substituted-1-en-3-one derivatives like 2-cyano-3,12-dioxooleana-1,9(11)-dien-28-oic acid (CDDO) as well as its C-28 methyl ester that were synthesized by Honda *et al.* (14). Expanding ring A system by incorporating an

 doi: 10.1111/cbdd.12380

azaheterocyclic ring at C-2/3 afforded hybrids with promising antiproliferative and apoptosis-inducing effects on hepatic carcinoma cells (BEL-7404) (15).

Breast tumor kinase (Brk), also called protein tyrosine kinase 6 (PTK6), is a ~60 kDa non-receptor protein kinase, which is highly expressed in approximately 86% of breast cancers, but minimally expressed in normal human mammary epithelial cells, suggesting a tumor cell-specific function (16). Brk activation and/or overexpression can promote proliferation, migration, and invasion of breast cancer cells in response to different ligands through multiple mechanisms. For instance, Brk mediates epidermal growth factor (EGF)-induced migration of breast tumor cells through a mechanism involving Ras-related C3 botulinum toxin substrate 1 (Rac1) mediated by paxillin (16). Paxillin, a multidomain cytoskeletal focal adhesion adaptor protein, acts as a molecular scaffold for other adaptors and structural proteins (17). Moreover, it mediates signal transduction and cross talk between adhesion and growth factor signaling (17). Paxillin has proven to regulate diverse physiological processes including gene expression, cell proliferation, adhesion, and motility (17). It is phosphorylated in response to numerous stimuli, including various growth factors such as insulin-like growth factor 1 (IGF-1), EGF, and hepatocyte growth factor (HGF). It is also a substrate for non-receptor tyrosine kinases such as focal adhesion kinase (FAK) (16). Rac1 is a member of the Rho GTPase family reported to play an essential role in cancer progression, invasion, and metastasis. Documented overexpression of Rac1 proteins was reported in most invasive human cancers, including metastatic breast cancer (16,17).

This study reports the discovery of oleanolic acid through bioassay-guided fractionation of *Terminalia bentzoe* L. leaves methanol extract as its principle breast cancer cell migration inhibitor. A series of five new (**9**–**12** and **15**) and seven known analogues were semisynthesized. All compounds were evaluated for their antiproliferative, antimigratory, and anti-invasive potentials against MDA-MB-231 human breast cancer cell line. We also report the discovery of Brk/Paxillin/Rac1 axis as a novel molecular target for the common dietary supplement triterpene oleanolic acid and analogues. Important structural pharmacophoric features of the active analogues were also deduced.

Methods and Materials

General experimental procedures

^{1}H and ^{13}C NMR spectra were recorded at 400 and 100 MHz, respectively, in appropriate deuterated NMR solvent, using TMS as an internal standard, on a JEOL Eclipse ECS-400 NMR spectrometer (Boston, MA, USA). The ESI-MS experiments were conducted using a 3200 Q-trap LC/MS/MS system (Applied Biosystems, Foster City, CA, USA) using ANALYST version 1.4.1 software (MDS Sciex, Toronto, ON, Canada). Si gel 60 (230–400 mesh; Natland International Corporation, Morrisville, NC, USA) was used for column chromatography, and analytical TLC was carried out on precoated Si gel 60 F_{254} TLC plates (EMD Chemicals Inc., Gibbstown, NJ, USA), using appropriate developing systems as reported for each experiment. TLC spots were visualized by spraying with a solution of freshly prepared *p*-anisaldehyde–ethanol–acetic acid–sulfuric acid (2:170:20:10 v/v) and heated at 105 °C until maximal spots color developed. All chemicals were purchased from Sigma-Aldrich (St. Louis, MO, USA) or Alfa Aesar (Ward Hill, MA, USA).

Plant material

Terminalia bentzoe L. (Combretaceae) leaves were collected at the Giza ZOO, Cairo, Egypt, in November 2012. A specimen was identified by Dr. Thérèse Labib, Taxonomy Specialist at Al Orman Botanical Garden Herbarium, Giza, Egypt. A voucher specimen (T.B. No. 1) was deposited at the Department of Pharmacognosy, Faculty of Pharmacy, Helwan University, Cairo, Egypt. The fresh leaves (5 kg) were dried in shade and grounded prior to extraction.

Extraction and bioassay-guided isolation

The dried leaves of *T. bentzoe* L. (1.5 kg) were extracted with methanol at 50 °C (7 L × 3). Extracts were combined and solvent was removed under reduced pressure at 50 °C to yield a brown viscous mass which was then lyophilized to give 250 g dry extract. Subsequent ultrasonication at room temperature with *n*-hexane (2 L × 3) and then acetone (3 L × 3) afforded hexane-soluble portion (5 g), acetone-soluble portion (94 g), and a residue (141 g). All were subjected to biological screening for their ability to inhibit migration of human breast cancer MDA-MB-231 cells in wound-healing assay (WHA) at different concentrations (25, 50, 100, 200 and 400 μg/mL). The bioactive acetone portion was then subjected to vacuum liquid chromatography on Si gel 60 eluted with *n*-hexane-CH_2Cl_2, CH_2Cl_2-EtOAc, and EtOAc-Me_2CO gradient systems by 50% increment/2 L. Fractions were pooled together based on their TLC similarity pattern affording four collective fractions. The most active cF_{III} eluted by CH_2Cl_2-EtOAc 5:5 to 0:10 was further purified by flash chromatography on Si gel 60 using gradient of CH_2Cl_2-EtOAc each with 10% increment/500 mL. Three triterpene acids were obtained: oleanolic **1** (CH_2Cl_2-EtOAc 8:2, 170 mg), masilinic **2** (CH_2Cl_2-EtOAc 6:4, 30 mg), and arjunolic **3** (CH_2Cl_2-EtOAc 2:8, 20 mg).

Semisynthetic reactions

Oxidation of oleanolic acid with CrO_3

To 2 mL solution of **1** (10 mg, 0.021 mmol) in toluene/acetone 4:1, an equimolar amount of CrO_3 was added (18). The reaction mixture was stirred for 1 h at room temperature after which 10 mL water was added to quench the reaction. The solution was then extracted with EtOAc

(10 mL × 3). The collected organic layers were dried over anhydrous Na_2SO_4 and evaporated. The residue was purified on Si gel 60 using *n*-hexane-EtOAc 8:2, isocratic system, to afford **4** (8 mg, yield 84%).

Carbamoylation of oleanolic acid

To solutions of **1** (20 mg, 0.043 mmol) in toluene (3 mL) was added an equimolar amount of different isocyanates and 10 μL of Et_3N (19). Each reaction mixture was refluxed with stirring at 110 °C for 2 h. Water (10 mL) was then added to quench the reaction followed by shaking with EtOAc (10 mL × 3). The combined organic layers were dried over anhydrous Na_2SO_4 and evaporated under vacuum. The solid residue was further purified on Si gel 60 column using gradient elution of *n*-hexane-EtOAc from 9:1 to 6:4, and fractions were collected each of 5 mL. **5** was eluted by *n*-hexane-EtOAc 8:2 (6 mg, yield 26%), **6** was eluted by *n*-hexane-EtOAc 8:2 (8 mg, yield 32%), **7** was eluted by *n*-hexane-EtOAc 7:3 (8 mg, yield 29%), **8** was eluted by *n*-hexane-EtOAc 8:2 (5.5 mg, yield 21%), **9** was eluted by *n*-hexane-EtOAc 7:3 (5 mg, yield 18%), **10** was eluted by *n*-hexane-EtOAc 7:3 (9 mg, yield 33%), **11** was eluted by *n*-hexane-EtOAc 7:3 (6 mg, yield 20%), and **12** was eluted by *n*-hexane-EtOAc 7:3 (6.5 mg, yield 23%).

Reaction of oleanolic acid with lead tetraacetate

To 20 mg (0.043 mmol) of **1** in 3 mL CH_2Cl_2, $Pb(OAc)_4$ (19.5 mg, 0.043 mmol) was added and stirred at room temperature for 48 h (20). The reaction was worked up by the addition of 10 mL water, followed by extraction with EtOAc (10 mL × 3). The combined organic layers were dried over anhydrous Na_2SO_4 and concentrated under vacuum. The residue was subjected to purification on Si gel 60 using gradient elution of *n*-hexane-EtOAc beginning with 9:1 to 7:3, to yield **13** (4 mg, yield 20%).

Reaction of oleanolic acid with *N*-bromosuccinimide

To 3 mL solution of **1** (10 mg, 0.021 mmol) in 20% aqueous acetone, *N*-bromosuccinimide (4 mg, 0.022 mmol) in 2 mL 20% aqueous acetone was added drop wise (21). The reaction stirred for 1 h then water (5 mL) was added, followed by extraction using EtOAc (5 mL × 3). Organic layers were collected, dried over anhydrous Na_2SO_4, and concentrated under vacuum. The residue was purified on Si gel 60 column eluted with *n*-hexane-EtOAc 7:3 isocratic system, to yield compound **14** (8.5 mg, yield 76%).

Reaction of compound 14 with *o*-chlorobenzenesulfonyl isocyanate

To solution of the lactone **14** (10 mg, 0.018 mmol) in 2 mL toluene stirred with one equivalent of *o*-chlorobenzenesulfonyl isocyanate (1.3 μL, 0.018 mmol) and 5 μL of Et_3N (19). The reaction mixture was refluxed with stirring at 110 °C for 2 h and worked up as in carbamoylation reaction. The solid residue (14 mg) was further purified on Si gel 60 column using gradient elution *n*-hexane-EtOAc from 8:2 to 6:4 with gradient increment of 10%, and fractions of 5 mL each were collected, affording compound **15** (*n*-hexane-EtOAc 7:3, 6 mg, yield 44%).

3-*O*-[*N*-(4′,5′,6′-trimethoxyphenyl)carbamoyl]-oleanolic acid (**9**): Reaction of **1** (20 mg, 0.043 mmol) with trimethoxyphenyl isocyanate (9.1 mg, 0.045 mmol), afforded **9**. White amorphous solid; ^1H and ^{13}C NMR (Tables 1 and 2); ESI-MS: *m/z* 664.4 $[M - H]^-$ (calcd. for $C_{40}H_{58}NO_7$).

3-*O*-[*N*-(benzenesulfonyl)-carbamoyl]-oleanolic acid (**10**): Reaction of **1** (20 mg, 0.043 mmol) with benzenesulfonyl isocyanate (5.7 μL, 0.043 mmol) was proceeded to give **10**. White amorphous solid; ^1H and ^{13}C NMR (Tables 1 and 2); ESI-MS: m/z 638.6 $[M - H]^-$ (calcd. for $C_{37}H_{52}NO_6S$).

3-*O*-[*N*-(3′-chlorobenzenesulfonyl)-carbamoyl]-oleanolic acid (**11**): Reaction of **1** (20 mg, 0.043 mmol) with 2-chlorobenzenesulfonyl isocyanate (6 μL, 0.043 mmol) was proceeded to give **11**. White amorphous solid; ^1H and ^{13}C NMR (Tables 1 and 2); ESI-MS: *m/z* 672.4 and 674.2 for $[M - H]^-$ and $[M + 2 - H]^-$, respectively, (calcd. for $C_{37}H_{51}ClNO_6S$).

3-*O*-[*N*-(5′-fluorobenzenesulfonyl)-carbamoyl]-oleanolic acid (**12**): Reaction of **1** (20 mg, 0.043 mmol) with 4′-fluorobenzenesulfonyl isocyanate (8 mg, 0.043 mmol) afforded **12**. White amorphous solid; ^1H and ^{13}C NMR (Tables 1 and 2); ESI-MS: *m/z* 656.6 $[M - H]^-$ (calcd. for $C_{37}H_{51}FNO_6S$).

3-*O*-[*N*-(3′-chlorobenzenesulfonyl)-carbamoyl]-12α-bromo-olean-28,13β-olide (**15**): White amorphous solid; ^1H and ^{13}C NMR (Tables 1 and 2); ESI-MS: *m/z* 750.4, 752.3, and 754.1 for $[M - H]^-$, $[M - H + 2]^-$ and $[M - H + 4]^-$, respectively, (calcd. for $C_{37}H_{50}ClBrNO_6S$).

Cell lines and culture conditions

The MDA-MB-231 human breast cancer cells were obtained from American Type Culture Collection (ATCC, Manassas, VA, USA). Cells were cultured in RPMI-1640 growth medium (Gibco®-Invitrogen, Grand Island, NY, USA) and 10% (v/v) fetal bovine serum (Lonza, Basel, Switzerland), supplemented with 2 mM L-glutamine, 100 IU/mL penicillin G, 100 μg/mL streptomycin, 25 μg/mL amphotericin B, 2.0 mg/mL $NaHCO_3$, 5.9 mg/mL HEPES, and maintained at 37 °C in humidified incubator under 5% CO_2.

The MCF-10A non-tumorigenic immortalized human mammary epithelial cells were purchased from American Type Culture Collection (ATCC). Cells were cultured in DMEM/F12 growth medium and 5% (v/v) horse serum,

Table 1: ^{1}H NMR spectroscopic data of compounds **9**–**12** and **15**[a]

	δ_H, mult. (*J* in Hz)				
Position	**9**	**10**	**11**	**12**	**15**
1	1.62, m	1.57, m	1.54, m	1.57, m	1.63, m
	1.04, m	0.90, m	0.90, m	0.91, m	1.01, m
2	1.70, m	1.53, m	1.50, m	1.53, m	1.54, m
3	4.47, dd (11.0, 4.6)	4.35, dd (10.0, 3.4)	4.34, dd (11.1, 4.7)	4.37, dd (14.6, 5.0)	4.38, dd (11.8, 5.0)
5	0.86, brs	0.73, brs	0.72, m	0.75, brs	0.80, m
6	1.51, m	1.45, m	1.46, m	1.49, m	1.46, m
		1.20, m	1.26, m	1.27, m	1.33, m
7	1.44, m	1.42, m	1.42, m	1.43, m	1.49, m
	1.30, m	1.25, m		1.26	1.37, m
9	1.55, m	1.49, m	1.45, m	1.51, m	1.68, m
11	1.84, m	1.85, m	1.84, m	1.84, m	1.62, m
12	5.27, brs	5.23, t (3.2)	5.23, brs	5.24, t (3.6)	4.24, brs
15	1.65, m	1.64, m	1.62, m	1.64, m	1.64, m
	1.32, m				1.16, m
16	1.58, m	1.60, m	1.57, m	1.60, m	2.12, m
	1.11, m				
18	2.81, dd (15.1, 5.0)	2.78, dd (13.7, 4.1)	2.78, dd (11.9, 3.6)	2.78, dd (14.6, 5.6)	1.96, m
19	1.60, m	1.59, m	1.54, m	1.61, m	2.28, m
	1.14, m	1.15, m	1.12, m	1.12, m	1.95, m
21	1.36, m	1.34, m	1.34, m	1.34, m	1.32, m
	1.20, m	1.19, m	1.18, m	1.20, m	1.24, m
22	1.78, m	1.77, m	1.75, m	1.78, m	2.30, m
	1.58, m	1.56, m		1.58, m	1.72, m
23	0.91, s	0.77, s	0.76, s	0.79, s	0.76, s
24	0.85, s	0.75, s	0.74, s	0.77, s	0.73, s
25	0.93, s	0.86, s	0.85, s	0.87, s	0.82, s
26	0.74, s	0.70, s	0.71, s	0.71, s	1.17, s
27	1.12, s	1.08, s	1.07, s	1.08, s	1.38, s
29	0.89, s	0.87, s	0.87, s	0.87, s	0.96, s
30	0.93, s	0.89, s	0.89, s	0.90, s	0.87, s
3′	6.68, s	7.95, dd (7.3, 1.3)		8.03, m	
4′		7.52, dd (7.5, 6.8)	7.55, m	7.21, dd (8.7, 8.2)	7.45, dd (7.8, 1.4)
5′		7.62, dd (7.3, 1.3)	7.53, m		7.56, dd, 8.2, 1.8)
6′		7.52, dd (7.5, 6.8)	7.44, dd (7.8, 6.8)	7.21, dd (8.7, 8.2)	7.53, dd (8.2, 7.8)
7′	6.68, s	7.95, dd (7.3, 1.3)	8.21, d (7.7)	8.03, m	8.21, dd (8.2, 1.8)
8′	3.83, s				
9′	3.78, s				
10′	3.83, s				

[a]In $CDCl_3$, 400 MHz, coupling constants (*J*) in Hz.

supplemented with 20 μg/mL EGF, 0.5 μg/mL hydrocortisone, 0.1 μg/mL cholera toxin, 10 μg/mL insulin, 100 IU/mL penicillin G, 100 μg/mL streptomycin, and incubated at 37 °C in humidified atmosphere of 5% CO_2.

Test compounds

Stock solutions (25 mM) of purified tested compounds were prepared in sterilized DMSO and stored at 4 °C. Working solutions at their final concentrations for each assay were prepared in appropriate culture medium immediately prior to use. The vehicle control (DMSO) was prepared by adding the maximum DMSO volume used to prepare test compounds to the convenient media such that its final concentration did not exceed 0.2% v/v. Standard oleanolic acid (purity ≥97%; Sigma-Aldrich) was considered as a positive control in all biological assays (11,15).

Migration assay

Wound-healing assay (WHA) was conducted as previously described (22). Briefly, the confluent monolayer MDA-MB-231 cells were harvested and seeded onto a sterile 24-well plate then allowed to attach overnight. A scratch wound was inflicted using a sterile 200-μL pipette tip. Wounds were photographed on an inverted microscope connected to vista vision camera to measure the boundary of the wound at premigration. Subsequently, cells were treated with different concentrations of test compounds in serum-starved media, each in triplicate, vehicle control was prepared by adding the maximum volume of DMSO used in preparing test compounds to serum-free media. Incubation was carried out for 20–24 h till wound was just about to close in control wells. Media was then aspirated, and cells were fixed by methanol prior to staining with Giemsa stain. Images were captured for each wound (3 images/well) and processed by

Table 2: ^{13}C NMR spectroscopic data of compounds **9**–**12**, **15**[a]

	δ_C, mult. (*J* in Hz)				
Position	**9**	**10**	**11**	**12**	**15**
1	38.1, CH_2	37.9, CH_2	37.9, CH_2	37.2, CH_2	37.9, CH_2
2	23.9, CH_2	23.4, CH_2	23.5, CH_2	23.4, CH_2	23.1, CH_2
3	82.6, CH	85.1, CH	85.2, CH	85.1, CH	84.8, CH
4	37.9, C	38.1, C	37.9, C	37.2, C	38.0, C
5	55.4, CH	55.2, CH	55.2, CH	55.2, CH	55.3, CH
6	18.2, CH_2	18.1, CH_2	18.1, CH_2	18.1, CH_2	17.5, CH_2
7	32.6, CH_2	32.5, CH_2	32.5, CH_2	32.5, CH_2	34.5, CH_2
8	39.3, C	39.2, C	39.3, C	39.2, C	42.6, C
9	47.6, CH	47.5, CH	47.5, CH	47.3, CH	45.5, CH
10	37.0, C	36.9, C	36.9, C	36.9, C	36.3, C
11	23.4, CH_2	23.4, CH_2	23.2, CH_2	23.4, CH_2	27.5, CH_2
12	122.6, CH	122.4, CH	122.4, CH	122.4, CH	56.1, CH
13	143.6, C	143.6, C	143.6, C	143.6, C	91.6, C
14	41.6, C	41.6, C	41.7, C	41.6, C	43.3, C
15	27.7, CH_2	27.7, CH_2	27.6, CH_2	27.7, CH_2	29.2, CH_2
16	23.0, CH_2	22.9, CH_2	22.9, CH_2	22.9, CH_2	21.3, CH_2
17	46.5, C	46.5, C	46.5, C	46.5, C	45.6, C
18	41.0, CH	41.0, CH	41.0, CH	41.0, CH	52.3, CH
19	45.9, CH_2	45.8, CH_2	45.8, CH_2	45.8, CH_2	39.9, CH_2
20	30.7, C	30.7, C	30.7, C	30.7, C	31.9, C
21	33.8, CH_2	33.8, CH_2	33.8, CH_2	33.8, CH_2	33.9, CH_2
22	32.4, CH_2	32.4, CH_2	32.4, CH_2	32.4, CH_2	30.4, CH_2
23	28.1, CH_3	27.9, CH_3	27.8, CH_3	27.9, CH_3	27.6, CH_3
24	16.8, CH_3	16.6, CH_3	16.6, CH_3	16.6, CH_3	16.4, CH_3
25	15.4, CH_3	15.4, CH_3	15.3, CH_3	15.4, CH_3	17.0, CH_3
26	17.2, CH_3	17.1, CH_3	17.0, CH_3	17.1, CH_3	19.1, CH_3
27	25.9, CH_3	25.9, CH_3	25.9, CH_3	25.9, CH_3	21.1, CH_3
28	182.7, C	182.9, C	182.0, C	182.0, C	179.5, C
29	33.1, CH_3	33.1, CH_3	33.1, CH_3	33.1, CH_3	33.3, CH_3
30	23.6, CH_3	23.6, CH_3	23.6, CH_3	23.6, CH_3	23.6, CH_3
1′	154.0, C	150.4, C	150.0, C	150.3, C	150.0, C
2′	134.1, C	138.7, C	136.0, C	134.5, C	136.0, C
3′	96.0, CH	128.2, CH	131.9, C	131.2, CH, d (9.5)	134.9, C
4′	153.4, C	129.0, CH	131.8, CH	116.3, CH, d (23)	131.8, CH
5′	134.7, C	133.9, CH	134.9, CH	134.9, C, d (260)	131.9, CH
6′	153.4, C	129.0, CH	127.2, CH	116.3, CH, d (23)	127.1, CH
7′	96.0, CH	128.2, CH	132.8, CH	131.2, CH, d (9.5)	132.9, CH
8′	56.1, CH_3				
9′	61.0, CH_3				
10′	56.1, CH_3				

C, quaternary; CH, methine; CH_2, methylene; CH_3, methyl carbons.
[a]In $CDCl_3$, 100 MHz, coupling constants (*J*) in Hz. Carbon multiplicities were determined by PENDANT experiment.

camera program (Liss View software, Radnor, PA, USA) where the healed wound width was measured. Percent migration was calculated using the following equation:

$$\text{Percent migration} = \frac{\text{wound width at zero time - wound width in treated well}}{\text{wound width at zero time - wound width in DMSO}} \times 100$$

The IC_{50} value for each compound was calculated by nonlinear regression of log concentration versus the % migration, implemented in GRAPHPAD PRISM version 5.0 (GraphPad Software, San Diego, CA, USA).

Proliferation assay

MDA-MB-231 cells were plated at a density of 1×10^4 cells per well (6 wells/group) in 96-well culture plates and allowed to adhere overnight for growth studies (23). The next day, cells were divided into different groups and then fed serum-free RPMI-1640 media supplemented with HGF as a mitogen and experimental treatments or vehicle-treated control media. Cells in all groups were fed fresh treatment media every other day for a 72 h treatment period. Viable cell count was determined using the MTT colorimetric assay. The absorbance was measured at λ 570 nm on a microplate reader (BioTek, Winooski, VT, USA). The number of cells per well was calculated against a standard curve

prepared at the start of the experiment. The IC_{50} value for each compound was calculated by nonlinear regression of log concentration versus the % survival, implemented in GRAPHPAD PRISM version 5.0 (GraphPad Software).

Invasion assay

The Trevigen's Cultrex® BME Cell Invasion Assay kit was used for assessment of anti-invasive activity against MDA-MB-231 cells[a]. The top invasion chamber was coated with 50 μL of basement membrane extract solution (1X BME) and incubated for 4 h at 37 °C in a 5% CO_2-humidified atmosphere. The coating solution was aspirated off, and 50 μL of cell suspension was added to each well at top chamber. Ten microlitre of tested compounds, prepared in serum-free medium, was added to each well in a final non-toxic concentration of 5 or 15 μM. About 150 μL of RPMI-1640 medium was added to lower chamber containing 10% FBS and fibronectin (1 μL/mL) and *N*-formyl-met-leu-phe (10 nM) as chemotactic agent and incubated at 37 °C in CO_2-humidified atmosphere for 24 h. Media were carefully aspirated from both chambers after which cell dissociation/calcein–AM solution was added to each bottom chamber well and incubated at 37 °C in CO_2 incubator for 1 h. The fluorescence of each sample was measured at 485 nm excitation and 520 nm emission by microplate reader (BioTek). The number of cells invaded per well was calculated against a standard curve prepared by plating various numbers of cells.

Cytotoxicity assay

The confluent monolayer MCF-10A cells were harvested and seeded into 96-well plate at density 2×10^4 cells/well and left to recover. Twenty-four hours postseeding, cells were treated with test compounds at different concentrations in fresh serum-free media, each in triplicate, and incubated at 37 °C in humidified atmosphere of 5% CO_2 for 24 h. At the end of treatment, media were replaced by fresh ones containing 50 μL MTT (1 mg/mL in PBS) and incubated for further 4 h. The insoluble formazan crystals were solubilized in 100 μL of DMSO, and absorbance was measured at 570 nm on microplate reader (BioTek). The average number of cells per well was calculated from the standard curve prepared by platting various cell concentrations at the start of the experiment.

Western blot analysis

MDA MD-231 cells were initially plated at a density of 1×10^6 cells/100-mm culture plate, allowed to attach overnight in RPMI-1640 media containing 10% FBS. Cells were then washed with 1X PBS and incubated with vehicle control or treatment in serum-free media supplemented with 20 ng/mL EGF as a mitogen for 3 days in culture (23). At the end of treatment period, cells were lysed in RIPA buffer (Qiagen Sciences Inc., Valencia, CA, USA). Protein concentration was determined by the BCA assay (Bio-Rad laboratories, Hercules, CA, USA). Equivalent amounts of protein were electrophoresed on SDS–PAGE, and the gels were electroblotted onto PVDF membranes and visualized according to the method described previously (23). The visualization of β-tubulin was used to ensure equal sample loading in each lane. All experiments were repeated at least three times, and a representative Western blot image from each experiment is shown in Figure 1.

Pharmacophore modeling

Pharmacophore modeling was carried out using PHASE (version 3.5, 2013) module of the Schrödinger suite implemented in Maestro (Maestro 9.3.5, 2012) molecular modeling package. The structures of compounds were built using the structure drawing tool and prepared using LigPrep (version 2.5, 2012). Conformers were generated using ConfGen by applying OPLS-2005 force-field method with implicit distance-dependent dielectric solvent model at cut-off root-mean-square deviation (RMSD) of 1 Å. A maximum of 500 conformers and 100 minimization steps were set. Compounds were divided into a training set of 12 compounds and a test set of three compounds using the leave-*n*-out method. The test set was used for the validation of the generated models. An arbitrary activity threshold value was then assigned to divide training set compounds into eight active (IC_{50} <15 μM) and six inactive ones (IC_{50} > 15 μM). Compounds **1**, **2**, **4**, and **13** were excluded as their inclusion limits the number of features in each hypothesis to hydrogen bond acceptors and hydrophobic groups only. Four features/sites were considered in generating pharmacophore variants: hydrogen bond acceptor

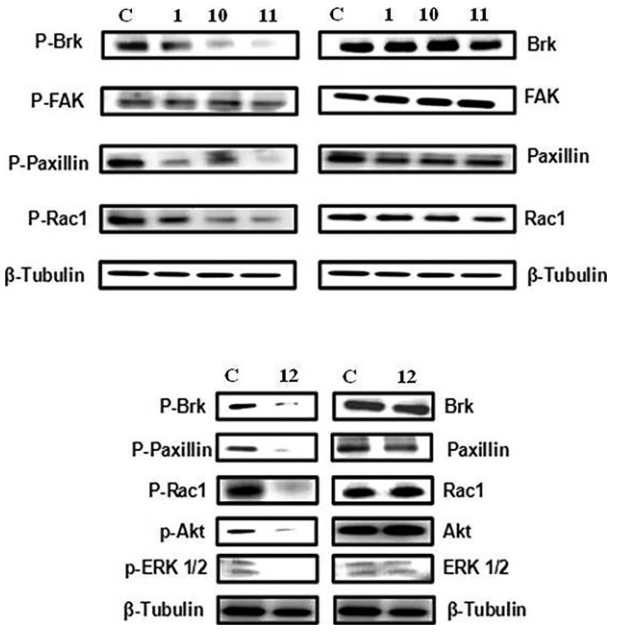

Figure 1: Oleanolic acid and active analogues **10**–**12** reduced Brk, paxillin, and Rac1 phosphorylation at 10 μM dose level evaluated by Western blot analysis.

(A), negative ionizable group (N), hydrophobic group (H), and aromatic ring (R). Resulting pharmacophore hypotheses were then scored using default weights of scoring parameters for both active (survival score) and inactive ones (survival-inactive scores). To further assist in ranking hypotheses, post hoc score was generated in which an activity reward was added for hypotheses that utilize the most active compound as the reference and a penalty assigned for hypotheses in which the reference ligand shows a high relative conformational energy. Hypotheses were clustered, and those with the highest survival score in each cluster were selected for further assessment. Four hypotheses were eventually selected: AAHHHR.165891, AAAHNR.322, AAHHNR.19590, and AAAHHR.808.

Statistical analysis

The results are presented as means ± SEM of at least three independent experiments. Differences among various treatment groups were determined by the analysis of variance (ANOVA) followed by Dunnett's test. A difference of $p < 0.05$ was considered statistically significant as compared to the vehicle-treated control group. The IC_{50} values represent concentrations that induce 50% cell growth, migration, and invasion inhibition.

Results and Discussion

Terminalia bentzoe L. leaves methanol extract showed a considerable antimigratory activity (IC_{50} = 200.0 μg/mL) against the human metastatic breast cancer cells MDA-MB-231 in WHA. Further fractionation by hexane and acetone followed by biological evaluation afforded active acetone-soluble portion with IC_{50} = 50.0 μg/mL. Subsequent bioassay-guided fractionation using vacuum liquid chromatography afforded a bioactive triterpene acid-rich fraction (IC_{50} = 7.3 μg/mL) identified from its 1D NMR spectra. The mixture was then subjected to further purification yielding three pure known triterpene acids: oleanolic (**1**), masilinic (**2**), and arjunolic (**3**) with their corresponding antimigratory IC_{50} at 14.0, 9.0, and >40.0 μM, respectively. The compounds were identified based on their spectroscopic analysis and comparing with literature (24–26).

Based on its high abundance in several plants and herbal remedies, oleanolic acid was chosen for further optimization. Diverse semisynthetic analogues of oleanolic acid (**1**) were prepared through reaction with chromium trioxide, different isocyanates, lead tetraacetate, and *N*-bromosuccinimide (NBS). Oleanolic acid was oxidized by CrO_3 (Scheme 1) to afford **4**, the corresponding 3-oxo-oleane-12-ene-28-oic acid (oleanonic acid) (15). Additionally, oleanolic acid was carbamoylated using various aromatic and olefinic isocyanates (Scheme 2) providing the expected C-3 carbamates **5**–**12**. Known carbamate analogues were identified as 3-*O*-[*N*-(allyl)-carbamoyl]-oleanolic acid (**5**), 3-*O*-[*N*-(benzyl)-carbamoyl]-oleanolic acid (**6**), 3-*O*-[*N*-(biphenyl)-*p*-carbamoyl]-oleanolic acid (**7**), and 3-*O*-[*N*-(2′-naphthyl)-carbamoyl]-oleanolic acid (**8**) based on their spectroscopic data and compared with literature (12). Compound **9** is the reaction product of oleanolic acid with 3,4,5-trimethoxyphenyl isocyanate. It exhibited in ESI-MS a molecular ion peak $[M - H]^-$ at *m/z* 664.4, suggesting the expected incorporation of the trimethoxyphenyl carbamoyl moiety to **1**. The ^1H and ^{13}C NMR data (Tables 1 and 2) revealed the downfield shift of H-3 to δ 4.47 and C-3 to δ 82.6, compared with the parent **1**, spotlighting the carbamoylation at position C-3. Additionally, the aromatic protons resonance at δ 6.68 (2H, s, H-3′ and H-7′) connected to its carbon at δ 96.0 in HMQC spectrum, suggested the expected trisubstituted phenyl ring. The aromatic methoxy singlets at δ 3.83 (6H, s) and 3.78 (3H, s) linked to their carbons at 61.0 and 56.1 ppm, respectively, in HMQC spectrum were attributed to 8′,9′,10′-trimethoxy pattern on the phenyl moiety. Therefore, analogue **9** was interpreted to be 3-*O*-[*N*-(8′,9′,10′-trimethoxyphenyl)-carbamoyl]-oleanolic acid. Compound **10** was furnished by the reaction of **1** with benzenesulfonyl isocyanate. Its molecular ion peak $[M - H]^-$ at *m/z* 638.6; with an increase of 181.9 a.m.u. than the parent (**1**); indicated inclusion of a benzenesulfonyl carbamoyl moiety. The ^1H and ^{13}C NMR data (Tables 1 and 2) along

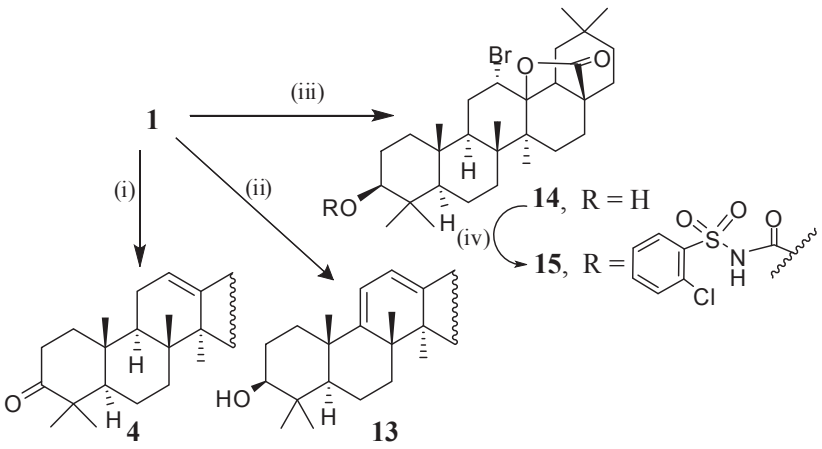

Scheme 1: Semisynthesis of **4** and **13**–**15**. (i) CrO_3, toluene/acetone, rt, 1 h. (ii) $Pb(OAc)_4$, CH_2Cl_2, rt, 48 h. (iii) *N*-bromosuccinimide, 20% aqueous acetone, rt, 2 h. (iv) R-N=C=O, Et_3N, toluene, reflux 110 °C, 2 h.

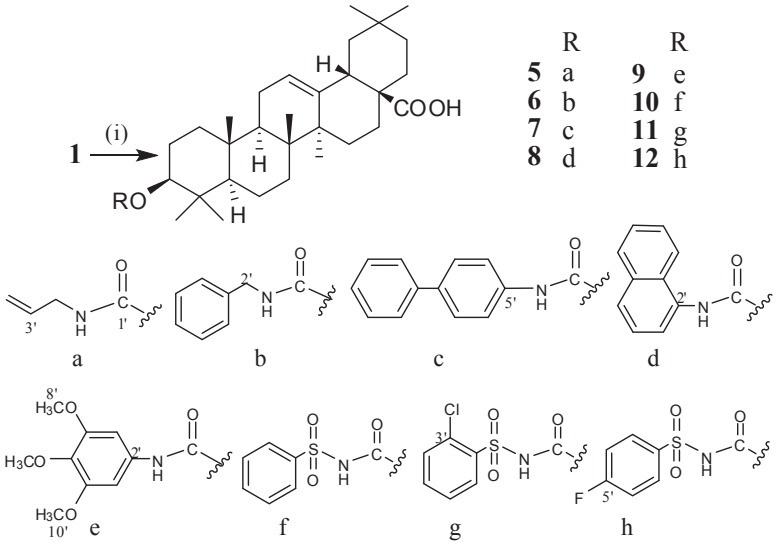

Scheme 2: Carbamoylation of oleanolic acid (**1**). (i) R-N=C=O, Et_3N, toluene, reflux 110 °C, 2 h.

with ^3J HMBC cross-peak between the carbamoyl carbon C-1′ (δ_C 150.4) and H-3 (δ_H 4.35) confirmed the carbamoylation at this position. Hence, **10** was interpreted as 3-*O*-[*N*-(benzenesulfonyl)-carbamoyl]-oleanolic acid. Compound **11** was obtained by the reaction of **1** with *o*-chlorobenzenesulfonyl isocyanate. Its ESI-MS spectrum displayed characteristic isotopic cluster signals of $[M - H]^-$ and $[M - H + 2]^-$ at *m/z* 672.4 and 674.2, respectively, with ratio 3:1, indicating a mono-chlorobenzenesulfonyl carbamate analogue. It exhibited similar ^1H and ^{13}C chemical shifts as **10** with 1,2-disubstituted benzene moiety of four aromatic protons [(8.21, 1H, d, *J* = 7.7), (7.55, 1H, m), (7.53, 1H, m), and (7.44, 1H, dd, *J* = 7.8, 6.8 Hz)] linked to their carbons in the HMQC spectrum at δ_C 132.8, 131.8, 134.9, and 127.2, respectively. Therefore, compound **11** was elucidated as 3-*O*-[*N*-(3′-chlorobenzenesulfonyl) carbamoyl]-oleanolic acid. Compound **12** is the reaction product of **1** with *p*-fluoro-benzenesulfonyl isocyanate. Its ESI-MS spectrum displayed a molecular ion peak $[M - H]^-$ at *m/z* 656.6, consistent with possible mono-fluorobenzenesulfonyl carbamate analogue of **1**. The ^1H and ^{13}C NMR data (Tables 1 and 2) showed the distinct splitting pattern for 1,4-disubstituted aromatic moiety due to coupling with the fluorine atom. The two aromatic protons (H-4′/6′) appeared as doublet of doublet with *J* = 8.7, 8.2 Hz due to the *ortho*-coupling with H-3′/7′ and fluorinated carbon C-5′. Their corresponding carbons at δ_C 116.3 displayed doublet splitting pattern (*J* = 23 Hz) as a result of ^2J coupling with C-5‘. The two aromatic carbons C-3′/7′ at δ_C 131.2 appeared as doublet (*J* = 9.5 Hz) were linked to their corresponding protons at δ_H 8.03 (2H, m) in HMQC spectrum. The assigned C-5′ at δ 165.9 splitted as doublet with *J* = 260 Hz due to ^1J-coupling with its *ipso*-fluoro atom. Thus, **12** was proved to be 3-*O*-[*N*-(5′-fluorobenzenesulfonyl)-carbamoyl]-oleanolic acid. Ring C modification was achieved by reacting **1** with $Pb(OAc)_4$ and NBS (Scheme 1) to afford compounds 3β-hydroxy-olean-9, 12-diene-28-oic acid (**13**), and 3β-hydroxy-12α-bromo-olean-28, 13-olide (**14**), respectively (27,28). Finally, for both ring C and C-3 modification, the lactone **14** was further reacted with *o*-chlorobenzenesulfonyl isocyanate to get **15** (Scheme 1). Its ESI-MS showed characteristic clusters for a mono-chlorinated, mono-brominated compound $[M - H]^-$, $[M - H + 2]^-$, and $[M - H + 4]^-$ at *m/z* 750.4, 752.3, and 754.1, respectively. The 1D NMR data (Tables 1 and 2) were comparable to **14** with few variations. Proton H-3 and carbon C-3 were downfield shifted by +1.19 and +5.7 ppm, respectively. It also showed a characteristic disubstituted benzene pattern [δ 8.21 (1H, dd, *J* = 8.2, 1.8 Hz), 7.56 (1H, dd, *J* = 8.2, 1.8 Hz), 7.53 (1H, dd, *J* = 8.2, 7.8 Hz), 7.45 (1H, dd, *J* = 7.8, 1.4 Hz)]. The HMBC spectrum showed cross-peak between the carbonyl C-1′ (δ 150.0) and proton H-3 (δ 4.38), confirming C-3 carbamoylation. Hence, **15** proved to be 3-*O*-[*N*-(3′-chlorobenzenesulfonyl)-carbamoyl]-12α-bromo-olean-28,13β-olide.

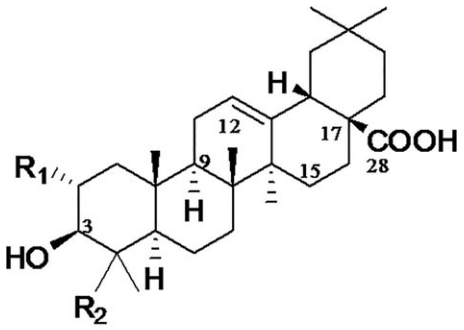

	R_1	R_2
1	H	CH_3
2	OH	CH_3
3	OH	α-CH_2OH

To study the *in vitro* inhibitory effect of oleanolic acid and its semisynthetic analogues against the human metastatic breast cancer cells MDA-MB-231, the scratch WHA has been conducted. Initially, to determine the activity role of the C-3 OH group, it was oxidized to a ketone **4**. Analogue **4** exhibited improved activity (IC_{50} = 5.5 μM, Table 3), versus its parent **1**, suggesting no hydrogen bonding donating role for C-3 OH in **1** for antimigratory activity. C-3 oxygen is likely to play a hydrogen acceptor role for this activity. Subsequently, a strategy was adopted for structure extension at C-3, maintaining the C-3 oxygen and diversifying the substitution to probe activity improvement. A series of various aromatic and olefinic carbamates were synthesized and tested. For instance, the benzyl carbamate analogue **6** exhibited IC_{50} = 17.0 μM, which was comparable to **1** (IC_{50} = 14.0 μM), while the olefinic allyl carbamate **5** was less active (IC_{50} > 40.0 μM), indicated that position C-3 can afford a carbamate moiety with medium bulkiness. To further assess the aromatic side chain size on the activity, the biphenyl carbamate **7** and the naphthyl carbamate **8** were synthesized and tested. Both analogues were less active (IC_{50} > 40.0 and 25.4 μM, respectively, Table 3) than the parent oleanolic acid, augmenting the preliminary observation of an optimal bulkiness of the phenyl moiety.

To explore the effect of different substituents on the phenyl moiety, the trimethoxyphenyl carbamate **9** was showing reduced antimigratory activity (IC_{50} > 40.0 μM, Table 3) indicating the unfavorable electron-donating group substitutions on the phenyl moiety. The effect of electron-withdrawing group substitutions at the phenyl carbamate moiety was also assessed. For instance, the benzenesulfonyl carbamate **10** showed enhanced activity, with an IC_{50} = 5.8 μM (Figure 2, Table 3). Comparing the activity of **10** and the benzyl carbamate **6**, the sulfonyl group's electron-withdrawing effect on the benzene ring improved the activity. This may be improving the carbamoyl NH group ionization at the physiological pH and possible generation of a salt bridge interaction within the binding pocket of the molecular target (29). The active benzenesulfonyl moiety was then maintained, and additional electron-withdrawing group substitution on the benzene ring at different positions was attempted. The *o*-chlorobenzenesulfonyl carbamate **11** showed nearly threefold more activity versus the unsubstituted carbamate **10** (IC_{50} = 2.1 μM, Figure 2). This suggested the importance of additional electron-withdrawing groups on the phenyl moiety. The *p*-fluorobenzenesulfonyl carbamate **12**

Table 3: IC_{50} (μM ± SEM) of natural triterpenes and semisynthetic oleanolic acid analogues in migration, proliferation, and cytotoxicity assays

Compound	Migration assay MDA-MB-231	Proliferation assay	Cytotoxicity assay MCF-10A
1	14.0 ± 2.4	11.2 ± 2.1	>50.0
2	9.0 ± 1.4	10.1 ± 0.6	30.2 ± 2.3
3	>40.0	56.1 ± 1.2	>50.0
4	5.5 ± 1.1	7.2 ± 1.3	>50.0
5	>40.0	18.0 ± 2.3	>50.0
6	17.0 ± 2.3	11.5 ± 0.7	15.5 ± 2.1
7	>40.0	26.6 ± 2.8	>50.0
8	25.4 ± 3.1	24.0 ± 2.2	29.4 ± 0.7
9	>40.0	18.9 ± 1.5	9.3 ± 0.6
10	5.8 ± 0.9	7.8 ± 0.6	4.5 ± 0.4
11	2.1 ± 0.5	6.1 ± 0.8	5.7 ± 1.1
12	1.4 ± 0.3	3.4 ± 0.4	17.7 ± 0.8
13	6.9 ± 1.1	8.1 ± 1.4	>50.0
14	>40.0	30.0 ± 3.2	4.0 ± 0.7
15	12.0 ± 2.0	9.7 ± 1.2	>50.0

Values representing the mean ± SEM of three independent experiments.

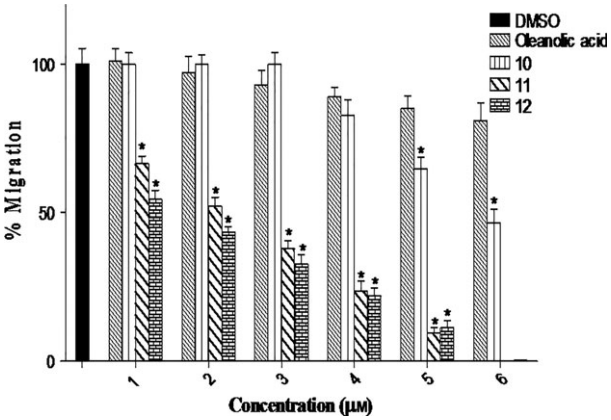

Figure 2: Effect of analogues **10**–**12** on MDA-MB-231 cell migration in wound-healing assay at different concentrations compared with DMSO as vehicle control. Oleanolic acid was used as positive control. Error bars indicate the SEM of n = 3 per compound. *p < 0.05.

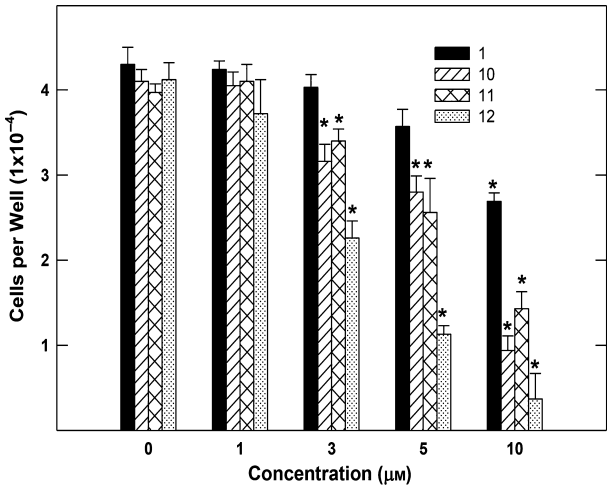

Figure 3: Effect of some active analogues on MDA-MB-231 breast cancer cells viability compared with DMSO as vehicle control and oleanolic acid as positive control. Error bars indicate the SEM of n = 3 per compound. *p < 0.05

exhibited nearly 10-fold enhancement in antimigratory activity, compared with **1** (Figure 2, Table 3). This clearly indicates the preference of small electron-withdrawing isostere on the phenyl moiety. Additionally, previous ring C modifications showed anticancer activity improvement of **1** (14). Therefore, $\Delta^{12,13}$ system was targeted through the use of NBS (Scheme 1), furnishing the unexpected bromolactone product **14**. This product offered the opportunity to test the importance of $\Delta^{12,13}$ system as well as the free COOH group for the antimigratory activity. Compound **14** was less active (IC_{50} > 40.0 μM) than **1**, pointing out the importance of intact $\Delta^{12,13}$ system and free COOH group. As benzenesulfonyl carbamoylation enhanced the activity of the parent **1**, compound **14** was further carbamoylated using *o*-chlorobenzenesulfonyl isocyanate to afford **15**. The latter regained the antimigratory activity, with an IC_{50} of 12.0 μM (Table 3), suggesting the ability of *o*-chlorobenzenesulfonyl carbamoylation to make up for the lost activity due to masking of the free C-28 COOH group, possible by offering additional binding pharmacophore at the molecular target. Additional unsaturation ($\Delta^{9,11}$) in ring C represented by **13**, which also reported as a natural product (eucalyptptanoic acid), showed enhanced antimigratory, with an IC_{50} of 6.9 μM (Table 3). This may suggest that the change in ring C geometry by additional unsaturation may offer better binding affinity to the molecular target, improving the overall bioactivity.

To assess the growth inhibitory effect of natural and semisynthetic triterpenes on MDA-MB-231 human breast cancer cells, the MTT (3-(4, 5-dimethyl-2-thiazolyl)-2, 5-diphenyl-tetrazolium bromide) proliferation assay was implemented (23). Oleanolic acid and some of its analogues significantly inhibited MDA-MB-231 cell growth in a dose-responsive manner as compared to vehicle-treated cells (Table 3). The natural products oleanolic (**1**) and masilinic (**2**) acids were both active with IC_{50} = 11.2 and 10.1 μM, respectively. Meanwhile, arjunolic acid (**3**) was nearly inactive, with an IC_{50} of 56.0 μM. This suggested C-2 hydroxylation has little effect on the activity of **2**, while hydroxylation of the C-23 methyl group greatly diminished the antiproliferative effect in **3**. The carbamate analogues displayed diverse activities, based on the size and nature of the side chain. The benzyl carbamate **6** maintained the antiproliferative activity (IC_{50} = 11.5 μM), while the allyl carbamate **5** was less active (IC_{50} = 18.0 μM). Therefore, analogous to migration, carbamates with aromatic side chain have more favorable antiproliferative activity than small olefinic moiety. Carbamates with more bulky chains as **7** and **8** showed reduced activity. In addition, carbamates with electron-donating substituents in the aromatic ring were less active than the benzenesulfonyl carbamates with *o*- or *p*-position small electron-withdrawing groups. Carbamate **12** with *p*-fluoro substituent was more active than *o*-chloro substituted carbamate **11** (IC_{50} = 3.4 and 6.1 μM, respectively), suggesting small electron-withdrawing group in *p*-position can better improve the antiproliferative activity. Demonstrated in Figure 3, the effect of various doses of oleanolic acid and most active analogues **10**–**12** on the viability of the human MDA-MB-231 mammary tumor cells after 3-day culture period.

Recently, the anti-invasive activity of oleanolic acid against malignant glioma cells was reported (11). Therefore, natural and semisynthetic triterpenes were further assessed for their ability to inhibit invasion of MDA-MB-231 breast cancer cells using Cultrex® BME cell invasion kit. Each compound was tested at subtoxic doses of 5 or 15 μM. Treatment with 5 μM oleanolic acid allowed 74% of cells to invade (Figure 4). Meanwhile, 5 μM treatments of the halogenated carbamates **11** and **12** allowed only 53.5 and 27.5% cell invasion, respectively. This indicated obvious anti-invasive activity improvement parallel to antimigratory activity. Other carbamates **6** and **15** were less active at

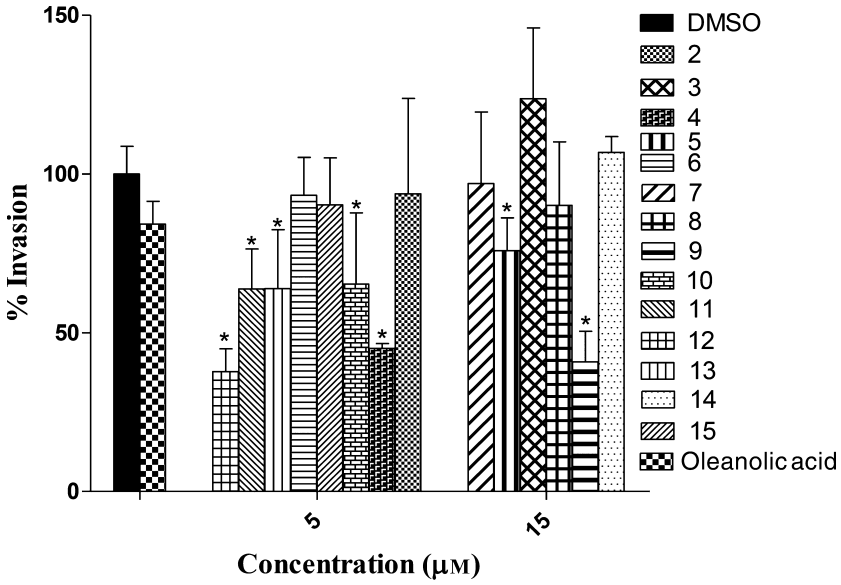

Figure 4: Anti-invasive activity of natural and semisynthetic triterpenes against MDA-MB-231 breast cancer cells using Cultrex® BME cell invasion assay. Oleanolic acid was used as positive control. Error bars indicate the SEM of n = 3 per compound. *p < 0.05.

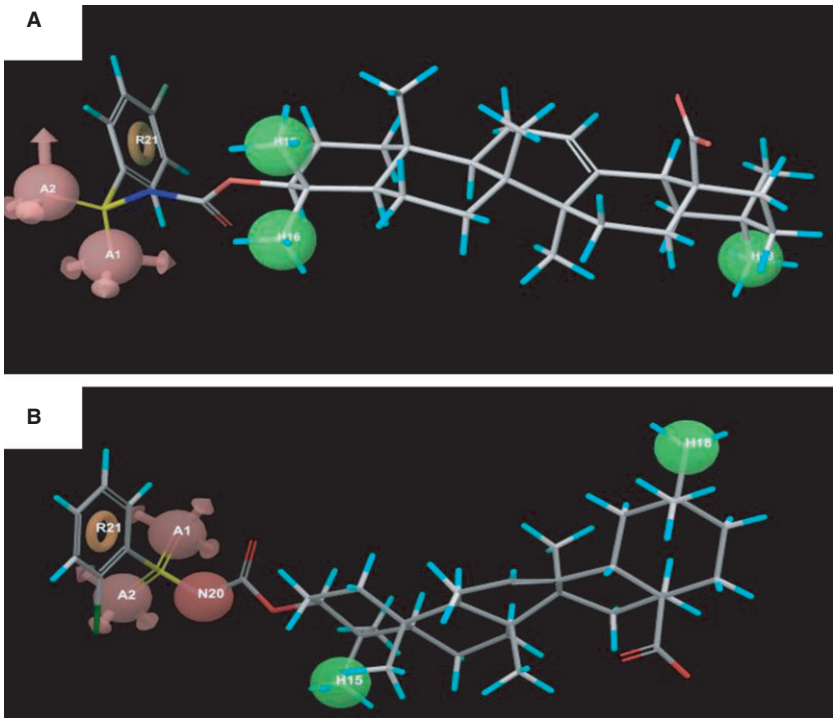

Figure 5: Alignment of active analogues. (A) analogue **12** aligned with the top-scoring hypothesis of variant AAHHHR. (B) analogue **11** aligned with the top-scoring hypothesis of variant AAHHNR. Light red spheres represent hydrogen bond acceptors (A), green spheres represent hydrophobic groups (H), dark red spheres represent negative ionizable groups (N), and brown ring represents aromatic group (R).

the same dose level, allowing 93.4 and 80.1% cell invasion, respectively. Carbamate **9** at 15 μM dose was allowing only 30% MDA-MB-231 cells' invasion, although it was inactive in migration assay.

The selective cytotoxicity of all tested natural and semisynthetic triterpenes toward the non-tumorigenic human mammary epithelial MCF-10A cells was assessed using MTT cytotoxicity assay. The results (Table 3) demonstrated that natural triterpenes and most semisynthetic analogues were non-toxic at relatively higher concentrations compared with their corresponding IC_{50} in different anticancer assays. For example, the most active analogue **12** showed an IC_{50} of 17.7 μM, while it exhibited IC_{50} values of 1.4 and 3.4 μM in migration and proliferation assays, respectively, against the breast cancer cells MDA-MB-231. These results clearly suggest the selectivity of **12** against the breast cancerous cells.

In an attempt to unravel the molecular signaling pathway that might justify the antimigratory and anti-invasive activities of oleanolic acid and related analogues, Western blot analysis was conducted. Treatment of human breast cancer MDA-MB-231 cells with 10 μM dose of oleanolic acid or its most active analogues (**10**–**12**) resulted in no effect on total Brk, paxillin, and Rac1 levels, whereas they resulted in a large reduction in phosphorylated (activated) Brk, paxillin, and Rac1 compared with vehicle-treated control groups. In addition, Western blot analysis showed that intracellular levels of FAK and p-FAK are similar in all treatment groups. Treatment with analogues **11** and **12** showed superior inhibition of phosphorylation (activation) of Brk/Paxillin/Rac1 signaling pathway (Figure 1). These results suggested that analogues **11** and **12** significantly blocked proliferation, migration, and invasion of the highly invasive MDA-MB-231 breast cancer cells. This effect might be related, at least in part, to the suppression of Brk/Paxillin/Rac1 signaling pathway. In addition, treatment with analogue **12** showed marked inhibition of phosphorylation (activation) of Akt and ERK1/2 which are important signaling molecules for survival and proliferation, respectively, without affecting their total levels.

Identification of the important structural pharmacophores required for the antimigratory activity of oleanolic acid

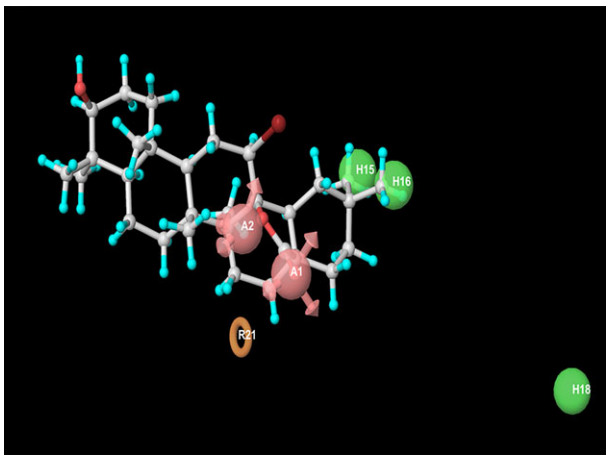

Figure 6: Poor spatial alignment of inactive analogue **14** with the pharmacophoric features. Light red spheres represent hydrogen bond acceptors (A), green spheres represent hydrophobic groups (H), and brown ring represents aromatic group (R).

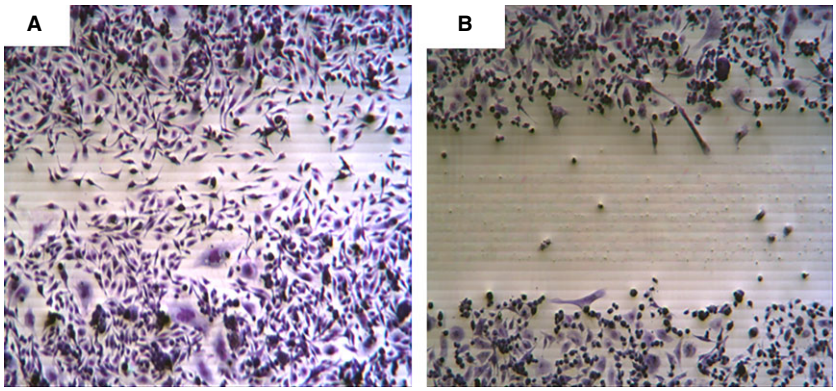

Figure 7: Antimigratory activity of analogue **12** against MDA-MB-231 breast cancer cells in WHA. (A) DMSO vehicle control. (B) 4 μM treatment of **12**.

analogues was achieved through a pharmacophore modeling study. PHASE module of the Schrödinger molecular modeling software was used, and a number of pharmacophore models were generated. A successful pharmacophore model identifies the important binding groups required for activity and their relative positions in space with respect to each other. Numerous common pharmacophore hypotheses (models) with different combination of variants (features) were generated.[b] Features explored in generating the hypotheses include hydrogen bond acceptor (A), negative ionizable group (N), hydrophobic group (H), and aromatic ring (R). Hypotheses were evaluated on the basis of survival, survival-inactive, and post hoc scores (30). Two-hundred hypotheses survived the scoring function; however, only the top-scoring hypothesis from each variant combination was selected including AAHHHR, AAAHNR, AAHHNR, and AAAHHR. These hypotheses showed superior alignment with active analogues (IC_{50} <15 μM, Figure 5), displayed lower relative conformational energy values for actives, and discriminated active and inactive analogues (lower fitness scores for inactive ones, IC_{50} > 15 μM, Figure 6) (30). The generated hypotheses further highlighted the most important structural features implicated in the antimigratory activity of oleanolic acid analogues, including C-X aromatic moiety and the sulfonyl carbamoyl group. The absence of any of these features significantly compromised the antimigratory activity. For example, the benzyl carbamate **6** is about twice as active as the allyl carbamate **5** but fourfold less active than the benzenesulfonyl carbamate **10**. In addition, carbamate **12** which verified most of the essential binding epitopes (Figure 5) showed the best antimigratory activity (Figure 7).

Conclusions

The common triterpene oleanolic acid from *T. bentzoe* L. was identified as the breast cancer cell migration inhibitor principle. Semisynthetic optimization of oleanolic acid afforded 12 analogues from which carbamate **12** showed potent selective antimigratory, antiproliferative, and anti-invasive activities against MDA-MB-231 cells at low μM level. Western blot analysis discovered Brk/Paxillin/Rac1 axis as a potential molecular target. Computer-aided pharmacophore modeling study correlated electron-deficient phenyl moiety at optimal bulkiness linked to a sulfonyl group as the main pharmacophores in active analogues. Based on the potent activity and selectivity, carbamate **12** is defined as a potential hit appropriate for further optimization for the use to control metastatic breast cancer.

Acknowledgments

The Egyptian Ministry of Higher Education and Helwan University, Cairo, Egypt, are greatly acknowledged for supporting H. E. Elsayed fellowship. The Louisiana Board of Regents is also acknowledged for supporting the new MS facility (LEQSF(2013-14)-ENH-TR-26).

Conflict of Interest

The authors of the present publication declare no conflict of interest.

References

1. Yi E.H., Lee C.S., Lee J.K., Lee Y.J., Shin M.K., Cho C.H., Kang K.W., Lee J.W., Han W., Noh D.Y., Kim Y.N., Cho I.H., Yel S.K. (2013) STAT3-RANTES autocrine signaling is essential for tamoxifen resistance in human breast cancer cells. Mol Cancer Res;11:31–42.
2. Cheng X., Hung M.C. (2007) Breast cancer brain metastases. Cancer Metastasis Rev;26:635–643.
3. Chambers A.F., Groom A.C., MacDonald I.C. (2002) Dissemination and growth of cancer cells in metastatic sites. Nat Rev Cancer;2:563–572.
4. Harvey A.L. (2008) Natural products in drug discovery. Drug Discov Today;13:894–901.
5. Mishra B.B., Tiwari V.K. (2011) Natural products: an evolving role in future drug discovery. Eur J Med Chem;46:4769–4807.
6. Owolabi M.S., Lawal O.A., Ogunwande I.A., Hauser R.M., Setzer W.N. (2013) Chemical composition of the

leaf essential oil of *Terminalia catappa* L. growing in south-western Nigeria. Am J Essent Oils Nat Prod;1:51–54.
7. Kinoshita S., Inoue Y., Nakama S., Ichiba T., Aniya Y. (2007) Antioxidant and hepatoprotective actions of medicinal herb, *Terminalia catappa* L. from Okinawa Island and its tannin corilagin. Phytomedicine;14:755–762.
8. Ramesh A.S., Christopher J.G., Radhika R., Setty C.R., Thankamani V. (2012) Isolation, characterisation and cytotoxicity study of arjunolic acid from *Terminalia arjuna*. Nat Prod Res;26:1549–1552.
9. Gurib-Fakim A., Demarne F. (1994) Essential oil of *Terminalia bentzoë* (L.) L. f. subsp. rodriguesensis Wickens. J Essent Oil Res;6:533–534.
10. Sultana N., Ata A. (2008) Oleanolic acid and related derivatives as medicinally important compounds. J Enzyme Inhib Med Chem;23:739–756.
11. Guo G., Yao W., Zhang Q., Bo Y. (2013) Oleanolic acid suppresses migration and invasion of malignant glioma cells by inactivating MAPK/ERK signalling pathway. PLoS ONE;8:e72079.
12. Ashour A., El-sharkawy S., Amer M., Abdel Bar F., Katakura Y., Miyamoto T., Toyota N., Bang T.H., Kondo R., Shimizu K. (2014) Rational design and synthesis of topoisomerase I and II inhibitors based on oleanolic acid moiety for new anti-cancer drugs. Bioorg Med Chem;22:211–220.
13. Pertino M.W., Lopez C., Theoduloz C., Schmeda-Hirschmann G. (2013) 1,2,3-Triazole-substituted oleanolic acid derivatives: synthesis and antiproliferative activity. Molecules;18:7661–7674.
14. Honda T., Rounds B.V., Gribble G.W., Suh N. (1998) Design and synthesis of 2-cyano-3,12-dioxoolean-1,9-dien-28-oic acid, a novel and highly active inhibitor of nitric oxide production in mouse macrophages. Bioorg Med Chem Lett;8:2711–2714.
15. Kang X., Hu J., Gao Z., Ju Y., Xu C. (2012) Synthesis, anti-proliferative and proapoptotic activity of novel oleanolic acid azaheterocyclic derivatives. Med Chem Com;3:1245–1249.
16. Chen H.Y., Shen C.H., Tsai Y.T., Lin F.C., Huang Y.P., Chen R.H. (2004) Brk activates Rac1 and promotes cell migration and invasion by phosphorylating paxillin. Mol Cell Biol;24:10558–10572.
17. Turner C.E. (2000) Paxillin and focal adhesion signaling. Nat Cell Biol;2:E231–E236.
18. Kim D.S., Pezzuto J.M., Pisha E. (1998) Synthesis of betulinic acid derivatives with activity against human melanoma. Bioorg Med Chem Lett;8:1707–1712.
19. El Sayed K.A., Khanfar M.A., Shallal H.M., Muralidharan A., Awate B., Youssef D.T., Liu Y., Zhou Y.D., Nagle D.G., Shah G. (2008) Latrunculin A and its C-17-*O*-carbamates inhibit prostate tumor cell invasion and HIF-1 activation in breast tumor cells. J Nat Prod;71:396–402.
20. Kyeremeh K., Baddeley T.C., Stein B.K., Jaspars M. (2006) A homologous series of eunicellin-based diterpenes from *Acalycigorgia* sp. characterised by tandem mass spectrometry. Tetrahedron;62:8770–8778.
21. Sawant S.S., Sylvester P.W., Avery M.A., Desai P., Youssef D.T., El Sayed K.A. (2004) Bioactive rearranged and halogenated semisynthetic derivatives of the marine natural product sarcophine. J Nat Prod;67:2017–2023.
22. Rodriguez L.G., Wu X., Guan J.L. (2005) Wound-healing assay. Methods Mol Biol;294:23–29.
23. Akl M.R., Ayoub N.M., Sylvester P.W. (2012) Mechanisms mediating the synergistic anticancer effects of combined γ-tocotrienol and sesamin treatment. Planta Med;78:1731–1739.
24. Seebacher W., Simic N., Weis R., Saf R., Kunert O. (2003) Complete assignments of ^{1}H and ^{13}C NMR resonances of oleanolic acid, 18α-oleanolic acid, ursolic acid and their 11-oxo derivatives. Magn Reson Chem;41:636–638.
25. Mahato S.B., Kundu A.P. (1994) ^{13}C NMR Spectra of pentacyclic triterpenoids–a complication and some salient features. Phytochemistry;37:1517–1573.
26. Bisoli E., Garcez W.S., Hamerski L., tieppo C., Garcez F.R. (2008) Bioactive pentacyclic triterpenes from the stems of *Combretum laxum*. Molecules;13:2717–2728.
27. Begum S., Sultana I., Siddiqui B.S., Shaheen F., Gilani A. (2002) Structure and spasmolytic activity of eucalyptanoic acid from *Eucalyptus camaldulensis* var. obtusa and synthesis of its active derivative from oleanolic acid. J Nat Prod;65:1939–1941.
28. Pungitore C.R., Garcia M., Gianello J.C., Sosa M.E., Tonn C.E. (2005) Insecticidal and antifeedant effects of *Junellia aspera* (Verbenaceae) triterpenes and derivatives on *Sitophilus oryzae* (Coleoptera: Curculionidae). J Stored Prod Res;41:433–443.
29. Carins D. (2008) Essentials of Pharmaceutical Chemistry, 3rd edn. London, UK: Pharmaceutical Press.
30. Dixon S.L., Smondyrev A.M., Knoll E.H., Rao S.N., Shaw D.E., Friesner R.A. (2006) PHASE: a new engine for pharmacophore perception, 3D QSAR model development, and 3D database screening: 1. Methodology and preliminary results. J Comput Aided Mol Des;20:647–671.

Notes

[a]Cultrex® BME Cell Invasion Assay Protocol. (2013) (www.trevigen.com, accessed December; 2013).
[b]Phase 3.5 Quick Start Guide. (2013) Schrödinger press, LLC.